

## Article

# Load-Settlement Characteristics of Stone Column Reinforced Soft Marine Clay Deposit: Combined Field and Numerical Studies

Sudip Basack <sup>1,2,\*</sup>  and Sanjay Nimbalkar <sup>3</sup> <sup>1</sup> Elitte College of Engineering, Affiliation: MAKU University of Technology, Kolkata 700113, India<sup>2</sup> Formerly, School of Civil, Mining & Environmental Engineering, University of Wollongong, Wollongong, NSW 2522, Australia<sup>3</sup> Geotechnical Engineering Division, School of Civil and Environmental Engineering, University of Technology Sydney, Sydney, NSW 2007, Australia; sanjay.nimbalkar@uts.edu.au

\* Correspondence: drsbasack@gmail.com; Tel.: +91-8617715761

**Abstract:** Foundations supporting infrastructure built on soft and compressible marine soil are unlikely to sustain due to possibility of undrained shear failure or excessive settlement of the supporting soil. This necessitates the importance of implementing an adequate ground improvement strategy. Among different techniques, soft soil reinforcing by the installation of stone columns is one of the most successful methods in terms of long-term stability of foundations. To investigate the load-settlement characteristics of such reinforced soil, a group of closely spaced stone columns was constructed at a location along the eastern coast of Australia. The site geology revealed thick layers of soft, compressible marine clay deposit. These stone columns were loaded by constructing earthen embankment and the resulting load-settlement characteristics were measured by an array of sensors. A two-dimensional plane strain analysis was performed using finite element modeling simulations. Comparison of numerical results with the field data demonstrated accuracy of the numerical model. Additional studies were carried out to investigate the efficiency of the model. This paper integrates the new findings from the full-scale field study and advanced numerical simulations while drawing pertinent conclusions.

**Keywords:** embankment; finite element model; marine clay; settlement; stone column reinforcement



**Citation:** Basack, S.; Nimbalkar, S. Load-Settlement Characteristics of Stone Column Reinforced Soft Marine Clay Deposit: Combined Field and Numerical Studies. *Sustainability* **2023**, *15*, 7457. <https://doi.org/10.3390/su15097457>

Academic Editors: Bernardino D'Amico, Suha Jaradat and Masoud Sajjadian

Received: 4 March 2023

Revised: 22 April 2023

Accepted: 25 April 2023

Published: 1 May 2023



**Copyright:** © 2023 by the authors. Licensee MDPI, Basel, Switzerland. This article is an open access article distributed under the terms and conditions of the Creative Commons Attribution (CC BY) license (<https://creativecommons.org/licenses/by/4.0/>).

## 1. Introduction

The strengthening of soft soils by installing stone columns is one of the most common ground improvement procedures applicable everywhere all over the world [1]. Numerous advantages include enhanced bearing capacity, settlement reduction, accelerated consolidation, and liquefaction control, to name a few [2]. The vertical drains filled with appropriate stone aggregates at the desired geometry are incorporated into the intended design [3,4].

Due to relative stiffness of the column and the soil, stress concentration occurs at the top of columns [5–7]. Due to their larger diameter and in addition higher hydraulic conductivity, the stone columns offer much rapid consolidation than prefabricated vertical drains and sand compaction piles [8]. In contrast to pile foundations, stone columns are effective and friendly to the environment [9].

Installation of stone columns induce significant disturbance in the surrounding soft soil, increasing its compressing and in turn reducing the permeability, the phenomena referred to as “smear” [10]. Arching occurs as a result of stress concentration, resulting in a parabolic vertical stress distribution on the loaded ground surface [11]. The radial flow predominates the vertical flow because of shortening of the drainage paths during consolidation [12]. A significant hydraulic gradient at the interface results in the washing out of fine clay particles into the pore spaces, gradually reducing the drainage area of the

stone columns, this phenomenon is referred to as “clogging” [13]. Whenever reinforced soft soil supports a transport infrastructure such as the railways or highways, the ground surface is subjected to cyclic loads apart from the usual static loads imposed by the regular traffic [14–16]. Significant experimental and numerical studies on stone column reinforced soft soil behavior were done in the recent past [17–22].

Limited research on field based study on stone column reinforced soft ground performance has been conducted in recent past [23,24]. Performance of reinforced ground under cyclic loading, which is quite relevant to the transport infrastructures, has been investigated by Ashour et al. [25].

The geometrical parameters of stone column reinforcement including diameter, depth of embedment, spacing and installation pattern depends upon various factors including the bearing capacity enhancement with settlement reduction, construction feasibility and cost effectiveness. Increased column diameter with reduced spacing is likely to enhance the bearing capacity with accelerated consolidation, but also will initiate constructional inconvenience and increased cost. When the soft clay deposit is extended to a relatively shallow depth overlying a stiff soil, the ideal situation would be to extend the stone columns covering the full soft soil layer and socketing to the stiff soil. For significant depth of soft clay, this would not be feasible, hence partially penetrated column would be installed. However, such an installation would retard the consolidation speed. Apart from these factors, the area replacement ratio is a key parameter to evaluate the stone column installation geometry [26–28]. The area replacement ratio ( $A_r$ ) is defined as [29],

$$A_r = [(r_e/r_c)^2 - 1]^{-1} \quad (1)$$

where,  $r_c$  and  $r_e$  are the radii of the column and its influence circle, respectively.

To explore the load-settlement characteristics of reinforced soft ground, a group of stone columns was installed in a soft, compressible marine clay deposit at a location along north-eastern coastal region in the state of New South Wales of Australia. To impart loads, a square earthen embankment is constructed on the reinforced ground surface in several stages. The resulting ground settlement was measured using a number of settlement plates installed for on-site monitoring during construction. Thereafter, a two-dimensional finite element analysis was carried out by PLAXIS<sup>2D</sup>. The numerical results are integrated and compared to field measurements for comprehensive interpretations and results with high credibility.

## 2. Motivation

It has been observed from the existing literature that knowledge gap exists in the current study area. Although significant volume of past contributions are available on laboratory model tests and theoretical (analytical and numerical) solutions, appropriate study of the instrumented field trial of the performance of stone column reinforced soft soil under embankment loading and its validation with adequate numerical model are quite limited. The current investigation has aimed to bridge-up this research gap.

## 3. Field-Based Investigation

A national soft soil field testing facility was established at a coastal site in the vicinity of the city of Ballina situated in the north-eastern coast of Australia in New South Wales [30]. The city of Ballina is located at the northeastern part of New South Wales, Australia close to the Queensland border. The geographical coordinates of the city have been 28.8628° S, 153.5658° E [31]. The current stone column site is located inside the National Soft Soil Testing Facility (NFTF) which is situated in the northwest of the city of Ballina, having an area of about 0.065 square kilometer [32]. The site is composed of soft, compressible, saturated marine silty clay that extends to an average depth of 10 m below the ground surface and is overlain by a stiff clay deposit [33]. The soft clay bed is overlaid by a 2 m thick remoulded crust layer composed of gravel and coarse sand with vegetative growth.

The installation site for the stone columns was located near the south-west corner of the entire field-testing site, as illustrated in Figure 1. The geotechnical properties of the marine clay are given in Table 1. A set of undisturbed samples of the Ballina clay were collected and tested in the laboratory. The moisture content and the dry unit weights of the soil varied in the ranges of 39–107% and 7–10 kN/m<sup>3</sup> [32,34]. From standard Proctor compaction tests, the optimum moisture content and the maximum dry density were derived as 38.5% and 13.9 kN/m<sup>3</sup>, respectively [35].

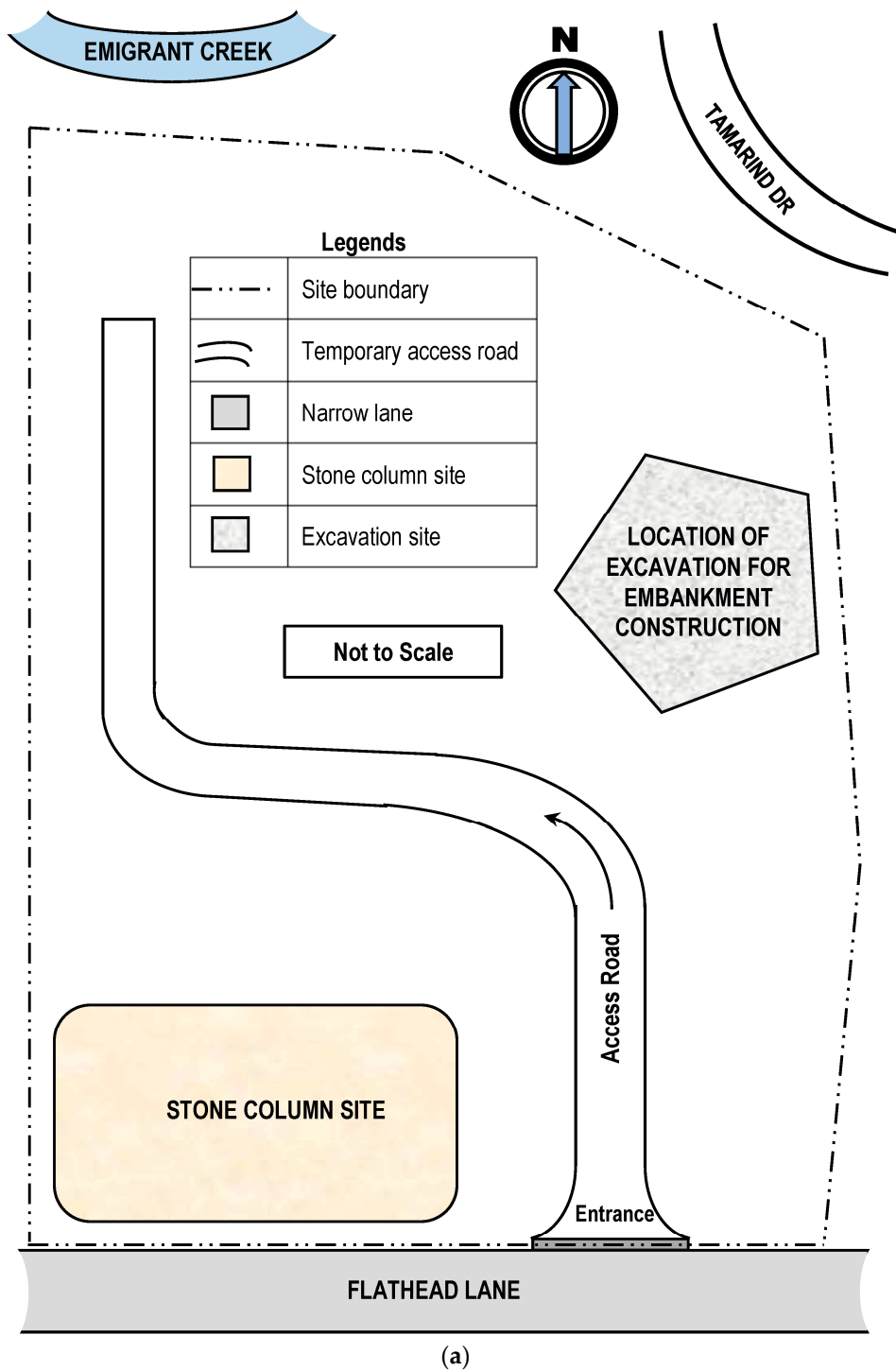
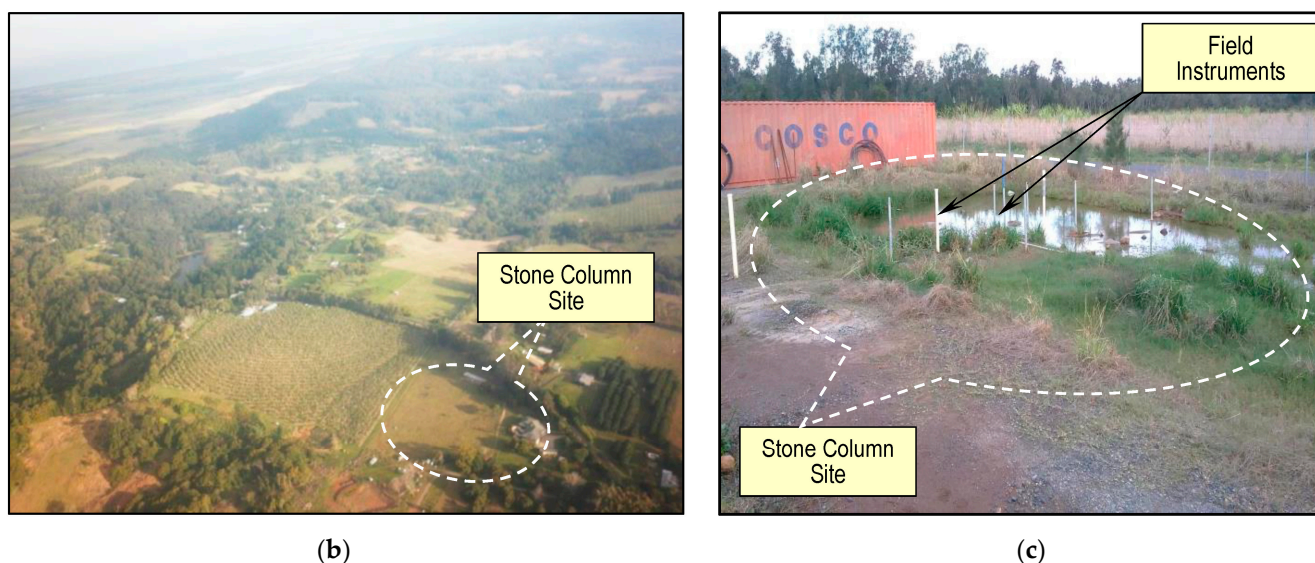


Figure 1. Cont.

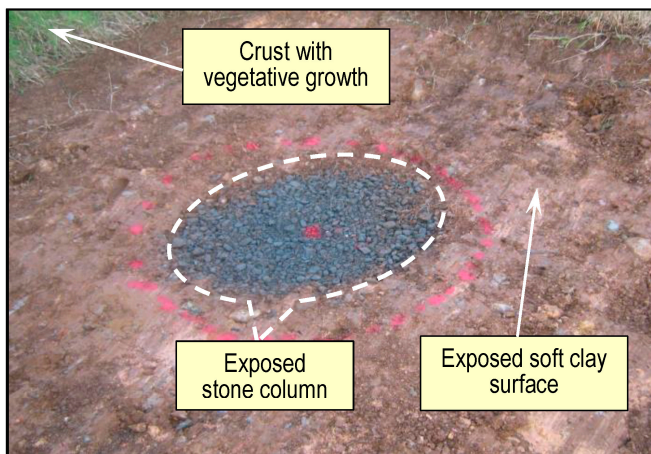
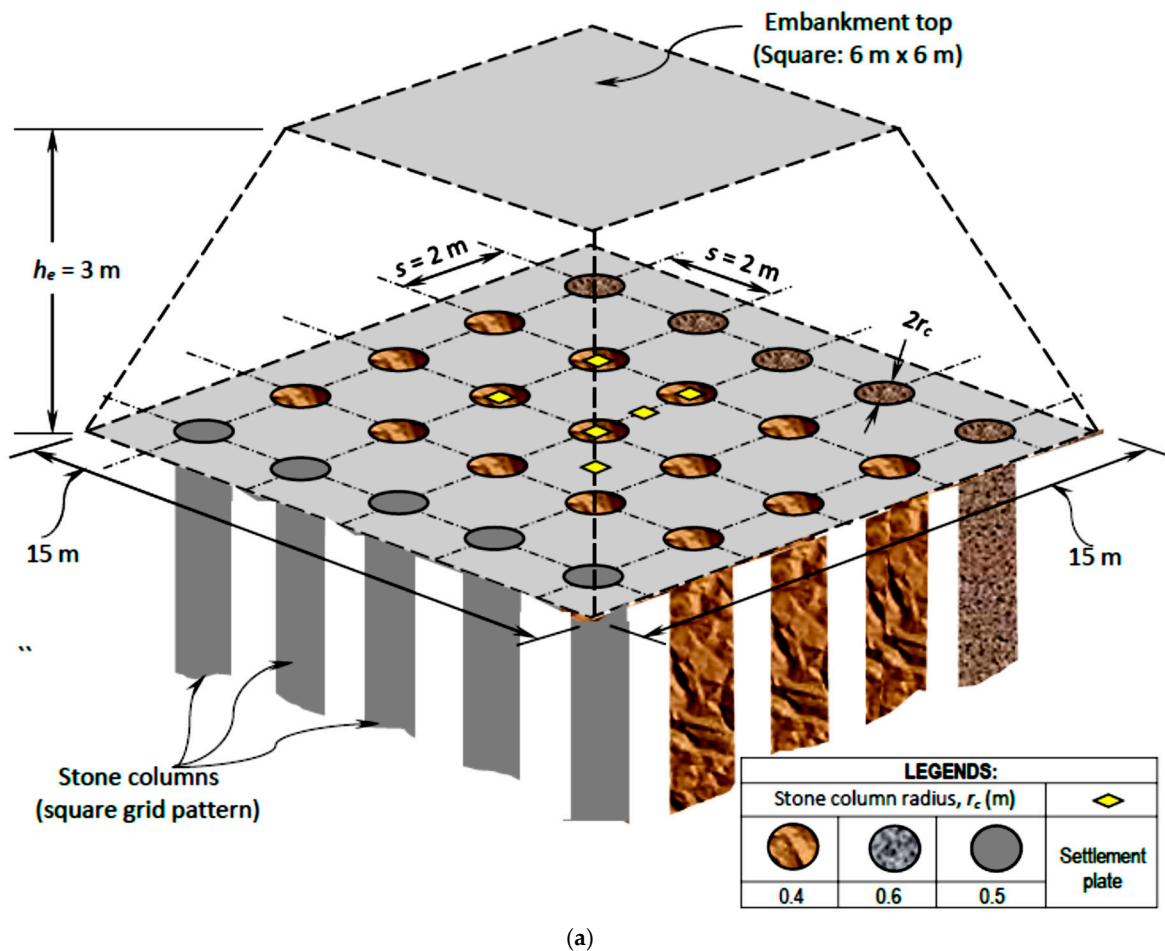


**Figure 1.** Characterization of the site location: (a) Sketch, (b) Oblique aerial view, and (c) On-site view (Photographs taken by Sudip Basack).

**Table 1.** Geotechnical properties of the soft marine clay deposit under investigation.

Parameter		Value	Unit
Average thickness of soft clay		10	m
Dry unit weight		7–10	kN/m <sup>3</sup>
Moisture content		30–107	%
Particle size distribution	Clay	78	%
	Silt	15	%
	Sand	7	%
Atterberg limit	Liquid limit	36	%
	Plastic limit	19.1	%
	Shrinkage limit	9.2	%
Standard Proctor Compaction test	Maximum dry density	13.9	kN/m <sup>3</sup>
	Optimum moisture content	38.5	%
Undrained shear strength parameters	Unit cohesion	2.5–20	kPa
	Friction angle	0	-
Consolidation parameters	Permeability	1.0–1.1	10 <sup>-9</sup> m/s
	Volumetric compressibility	5.0–5.1	10 <sup>-5</sup> m <sup>2</sup> /N

A total of 50 ( $=5 \times 10$ ) stone columns were installed by Keller Ground Engineering at the site in a square grid pattern, with the target diameters of 0.8 m, 1 m and 1.2 m, as shown in Figure 2. The selected installation method was wet vibro-replacement method. The stone columns were installed up to a depth of 10.5 m below the ground surface. A set of field instruments were installed thereafter including a group of settlement plates. A layer of angular railway ballast with an average size of 40–80 mm was placed and compacted on the geotextile layer, resulting in a finished ballast layer with an average thickness of 1 m. Thereafter, a sand blanket with an average thickness of 50 mm was placed on the top of the finished ballast layer.



(b)



(c)

**Figure 2.** (a) Sketch of stone column reinforcement and embankment, (b) exposed stone column, and (c) embankment (Photographs taken by Sudip Basack).

The embankment was thereafter constructed using silty sand reclaimed from a nearby local site and compacted at optimum moisture content. The embankment base was measured as 15 m  $\times$  15 m square, with a 3 m height and a 1.5 H:1 V side slope, resulting in a 6 m  $\times$  6 m square top surface. The construction sequences are portrayed in Figure 3, while the construction work in progress including the excavation and filling of embankment material is depicted in Figure 4. The engineering properties of different materials are presented in Table 2.

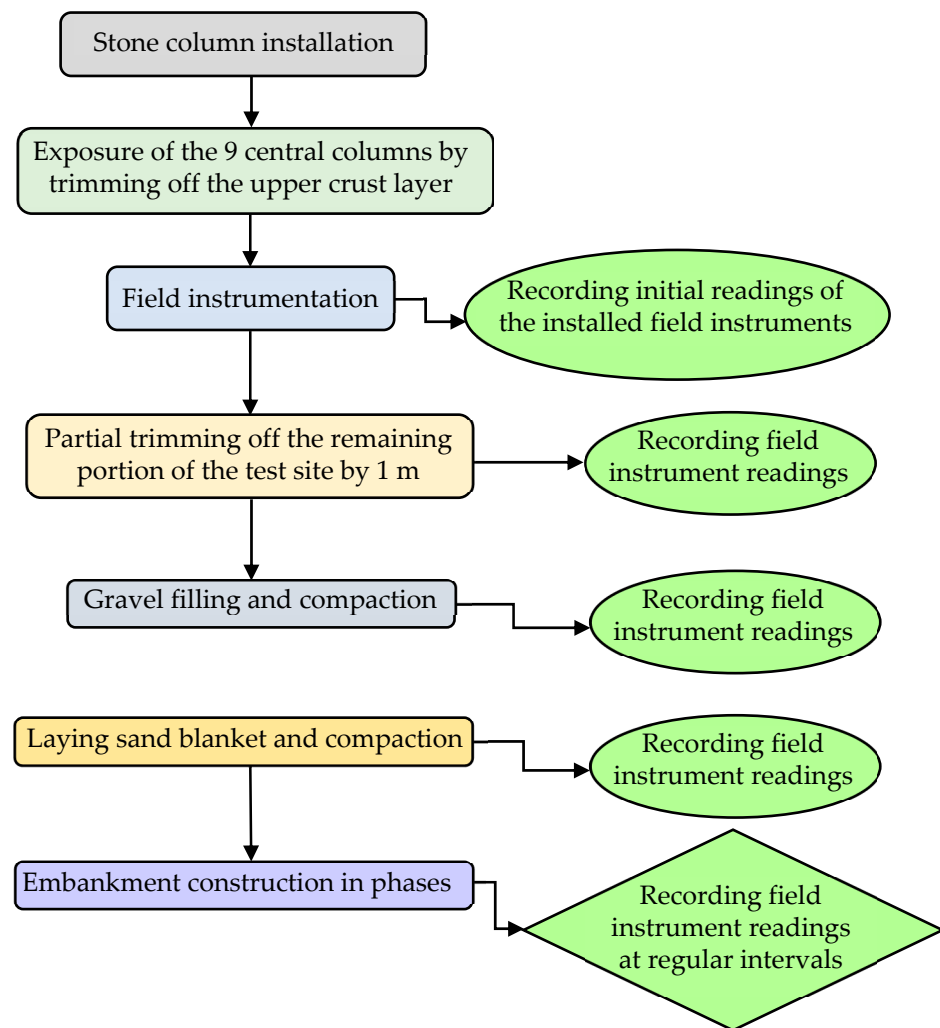


Figure 3. Flowchart for the stages of field construction.

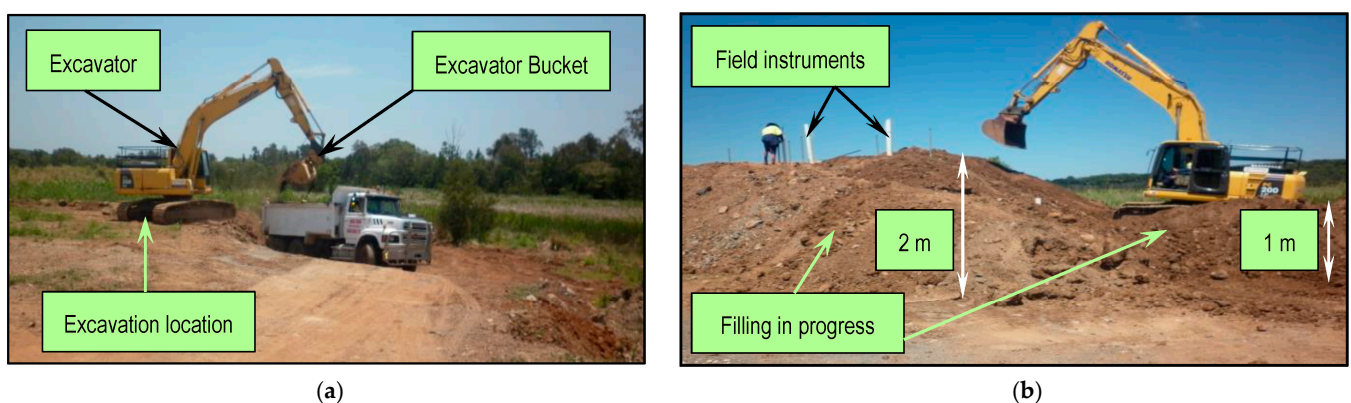


Figure 4. Photographic views of construction in progress: (a) excavation of embankment material, and (b) filling for embankment construction (Photographs taken by Sudip Basack).

The records of the settlement plates were obtained at regular intervals, from the commencement of construction. The measurements were taken using the precise and convenient Geographical Positioning System (GPS) survey technique. The data acquired by the system were more reliable and accurate compared to the other manual methods, for example, the theodolite technique. More details of the field-based investigation can be obtained from the previous works [36,37].

**Table 2.** Geotechnical properties of different field materials.

Material	Parameter	Value	Unit	
Embankment	Bulk unit weight	21.1	kN/m <sup>3</sup>	
	Moisture content	21.5	%	
	Particle size distribution	Clay	5	%
		Silt	40	%
		Sand	30	%
		Gravel	25	%
	Standard Proctor compaction test	Maximum dry density	17.86	kN/m <sup>3</sup>
Optimum moisture content		22.23	%	
Drain shear strength parameters	Unit cohesion	5	kPa	
	Friction angle	38	°	
Sand blanket	Average particle size	0.6	mm	
	Dry unit weight	20	kN/m <sup>3</sup>	
	Friction angle (direct shear test)	32	°	
Gravel fill	Particle size	40–80	mm	
	Friction angle (direct shear test)	42	°	
	Dry unit weight	22.76	kN/m <sup>3</sup>	
Crust	Particle size distribution	Clay	22	%
		Silt	23	%
		Sand	37	%
		Gravel	18	%
	Unit weight	Bulk	14.67	kN/m <sup>3</sup>
		Dry	11.2	kN/m <sup>3</sup>
	Friction angle (direct shear test)	29	°	
Natural moisture content	31	%		

Note: °: It is angular measurement and it is Degree.

The data presented in Tables 1 and 2 above have been obtained by collecting undisturbed samples from the site from selected locations and carrying out laboratory tests following the procedures standardized by American Society for Testing of Materials (ASTM).

#### 4. Finite Element Analysis

The two-dimensional (2D) plane strain finite-element modeling (FEM) simulations are performed by employing the finite-element program PLAXIS<sup>2D</sup> [38], which is based on Biot's consolidation theory. The PLAXIS program is used to mimic the cross section of the embankment resting on stone column stabilized clays at the site. The granular fill is considered to be free-draining. At a depth of 30 m below the ground surface, the boundary displacements are fully restricted. The model is laterally expanded by 60 m to mitigate the impact of lateral boundaries. In the area adjacent to the soil-column interface, a finer mesh size is utilized. Figure 5 depicts the FEM discretized mesh and boundary conditions of the embankment. The discretization process employs a total of 10,904 triangular 6-noded elements with six displacement nodes and three pore pressure nodes. At the left and right boundaries, roller supports are used to constrain the horizontal movement and to simulate smooth vertical contact. The bottom boundary is completely fixed and impermeable whereas the top and outer boundaries are permeable, allowing drainage in the horizontal direction towards the stone column to be facilitated.

The water table is assumed to be at the ground surface, and the  $K_0$  procedure is used to replicate the initial stress state in the ground.

In the finite element modeling, a plane strain analysis has been adopted with respect to the central cross section of the embankment. For a square embankment with square pattern of stone column installation in the field, such analysis is symmetrical with respect to the chosen central plane. Thus, the average deviation of numerical results with the field data is low (about 10%), as discussed later. Although more accurate numerical results

would have been obtained by a 3D finite element analysis, this would require enormous computational effort with significantly high computational time and hard disc memory usages, without much improvement in the accuracy of numerical results compared to a 2D analysis [39,40]. In the current analysis, the PLAXIS<sup>2D</sup> version 2017 has been used for the modeling [38].

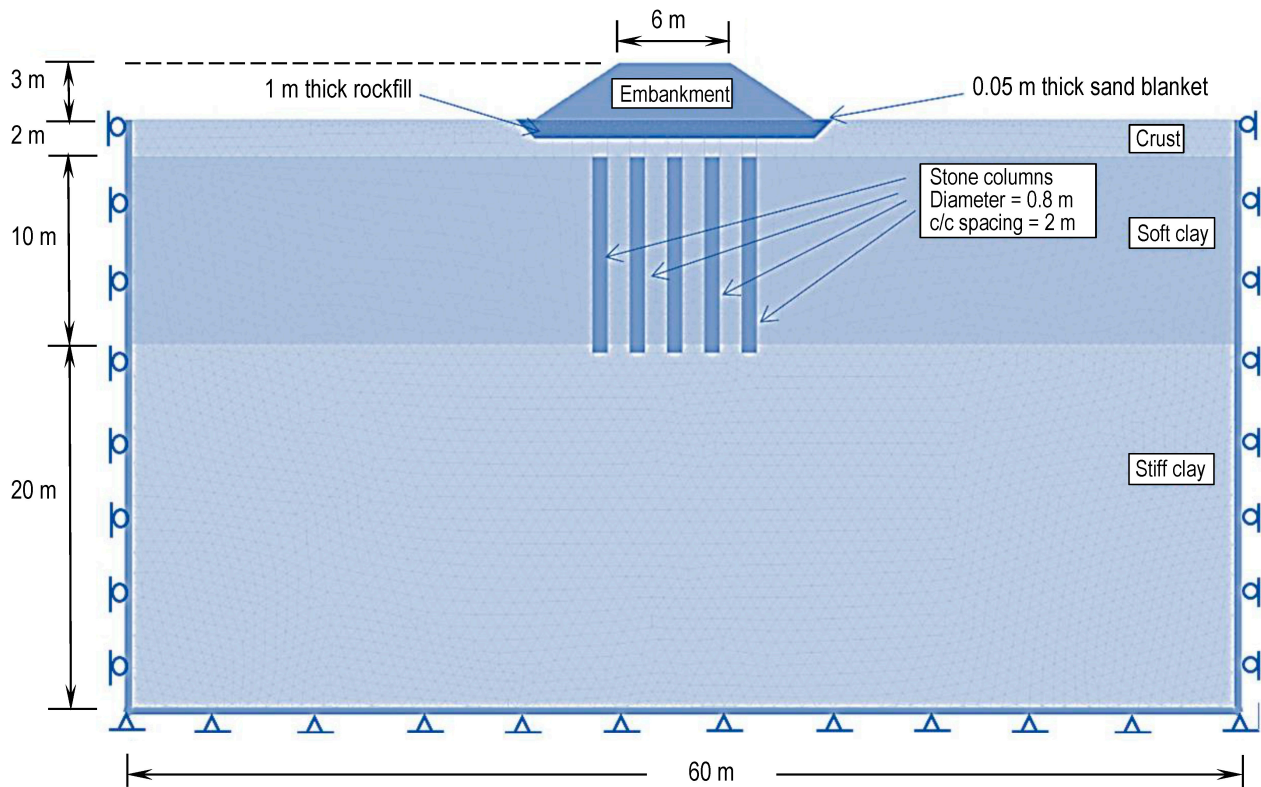


**Figure 5.** Finite element discretized mesh and boundary conditions.

In the finite element analysis, the soft soil (SS) model is applied to simulate the responses of soft normally consolidated clays. The SS model is required to address the shortcomings of its predecessor models in terms of capturing the time-dependent behaviour of soft soils [38]. The stiff silty clay layer that lies under the column-improved region is likewise modeled using SS model, as this layer is found to be roughly identical to normally consolidated clay. Hardening soil (HS) model is employed to imitate stone columns. Mohr-Coulomb is used for the granular fill materials, such as, embankment fill, sand blanket, gravel fill and top compacted crust materials.

During installation, the soil in the vicinity of the column surface is likely to be disturbed, reducing its permeability and compressibility. This phenomenon has been termed as “smear”, while the zone of disturbance is called “smear zone”. Due to reduction in permeability and compressibility, the consolidation is retarded to some extent, affecting the ground settlement rate [41]. Several past contributions on finite element analyses of stone column reinforced soft ground performance did not consider the smear zone effects [42–44]. In the current model, on the other hand, the interface elements have been modeled with reduced permeability and compressibility parameters by introducing an interface reduction factor ( $R_{int}$ ). Using such reduced parameters, the smear zone effect has been indirectly incorporated in the numerical model. With such technique, the numerical results were found to closely match with the field observations, as discussed in details later. The relevant expression of the equation can be presented as follows [45]:

$$P_r = R_{int}P_u \quad (2)$$

where,  $P_u$  and  $P_r$  are the undisturbed and reduced parameters, respectively.

Whenever a stone column reinforced soft clay deposit is subjected to embankment loading on the ground surface, initially the entire load is borne by the soft soil. As consolidation proceeds, settlement of the ground surface gradually takes place and the load sharing on the column progressively increases. In such process, the entire soft clay surface arches over the column, the phenomenon being termed as arching. Detailed analytical and numerical analyses with appropriate mathematical formulations on the arching effect were conducted by the author earlier [12,15]. In the current finite element model, on the other hand, the load sharing on column and soil was incorporated by default. The PLAXIS 2D model was set up in such a manner that the time dependent load sharing was automatically simulated in the software so as to yield the load-settlement characteristics of reinforced soft ground surface.

In the field, stone column installations are mostly implemented using the vibro-replacement methods which may be wet or dry [46]. Such installation produces radial displacements of the stone particles under high pressure which alter the surrounding soft soil characteristics and affect the load-settlement characteristics and bearing capacity of the improved soil [47]. In the current numerical model, the parameters of soft soil, stone column and interface have been chosen in a way that the installation effect is indirectly incorporated in the finite element analysis yielding the numerical results close to the field observations. However, it is true that for a more rigorous analysis, a 3D modelling with spatial variation of soil, column and interface parameters would be required, but this may require enormous computational effort. This section may be divided by subheadings. It should provide a concise and precise description of the experimental results, their interpretation, as well as the experimental conclusions that can be drawn.

Further details of the mathematical background of the soil-column system performance under embankment loading are added herein below.

#### 4.1. Mathematical Background

The primary function of stone columns is to act as a soil reinforcement, because of their greater stiffness compared the surrounding soft soil. The stress concentration ratio ( $n_s$ ) is given as,

$$n_s = \sigma_c / \sigma_s \quad (3)$$

where,  $\sigma_c$  and  $\sigma_s$  are the vertical stresses of the corresponding nodes of column and soil in the vicinity of the interface.

The behavior of the system comprising of stone column, soil and embankment is largely dominated by radial (inward towards the columns) consolidation. The Barron's theory of radial consolidation [48] holds good. This is given by:

$$\nabla_t u = c_{vr} \nabla_r^2 u \quad (4)$$

where,  $\nabla_t \equiv \frac{\partial}{\partial t}$ ,  $\nabla_r^2 \equiv \frac{1}{r} \frac{\partial}{\partial r} + \frac{\partial^2}{\partial r^2}$ ,  $u$  is the nodal excess pore water pressure and  $c_{vr}$  is the coefficient of radial consolidation.

There shall also be minor vertical component of consolidation, given by [5]:

$$\nabla_t u = c_{vz} \nabla_z^2 u \quad (5)$$

where,  $\nabla_z^2 \equiv \frac{\partial^2}{\partial z^2}$  and  $c_{vz}$  is the coefficient of vertical consolidation.

Under embankment loading, the initial imposed load is entirely taken care of by the pore water. As consolidation progresses, the vertical stress on the column gradually increases. Thus, the stress concentration ratio is essentially time dependent [8].

The settlement analysis of ground surface was obtained from the following correlation:

$$\rho_a^t = [2(r_e^2 - r_c^2)^{-1}] \int_{r_c}^{r_e} \int_0^H \int_0^t m_v \nabla_t u \, r \, dr \, dz \, dt \quad (6)$$

where,  $\rho_a^t$  is the average ground settlement at time  $t$ ,  $r_c$  and  $r_e$  are the radii of column and its influence area,  $m_v$  is the soil volumetric compressibility,  $r$  and  $z$  are the radial and depth coordinates, respectively.

#### 4.2. Initial and Boundary Conditions

In the finite element model, the soil boundaries considered are 30 m along horizontal direction from the embankment centerline while 30 m below the soft clay surface. Thus, the sufficiently wide boundaries significantly reduce the possibilities of influencing the computed results (for more explanation, see [39,49]). The side boundaries are chosen under roller-supports, eliminating any frictional resistance against vertical displacement. The bottom boundary, on the other hand, has been assumed to be hinge-supported, which prevented rotational restraint.

### 5. Results and Discussion

#### 5.1. Results

The average ground settlement around the central column was determined by taking the arithmetic mean of the values of ground settlement derived from the six settlement plates. The variation of the measured and the numerically predicted average ground settlement with time is depicted in Figure 6. During the first 80 days since commencement of loading, the measured and predicted values of average ground settlement varied between 0–71 mm and 0–79 mm, respectively, with the predicted values primarily on the higher side. As observed, the settlement increases with time following a nonlinear pattern, which is consistent with the loading being imposed on the ground surface in stages. The numerical values of settlement are in a considerable agreement with the measured values, with an average deviation of about 10%.

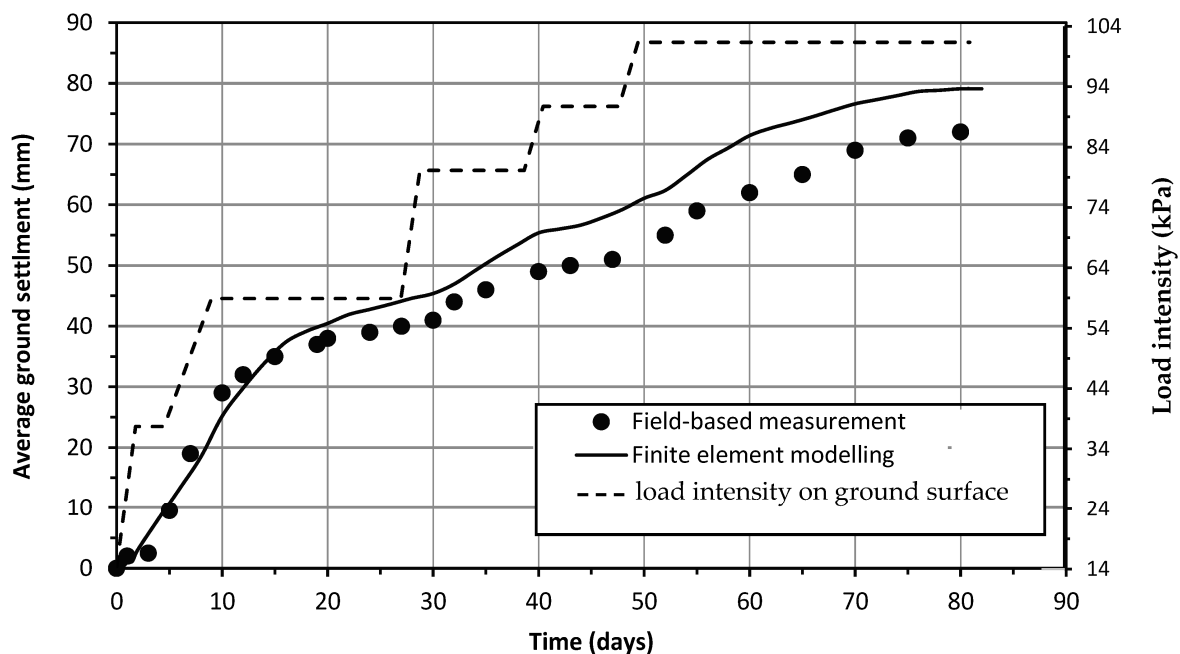
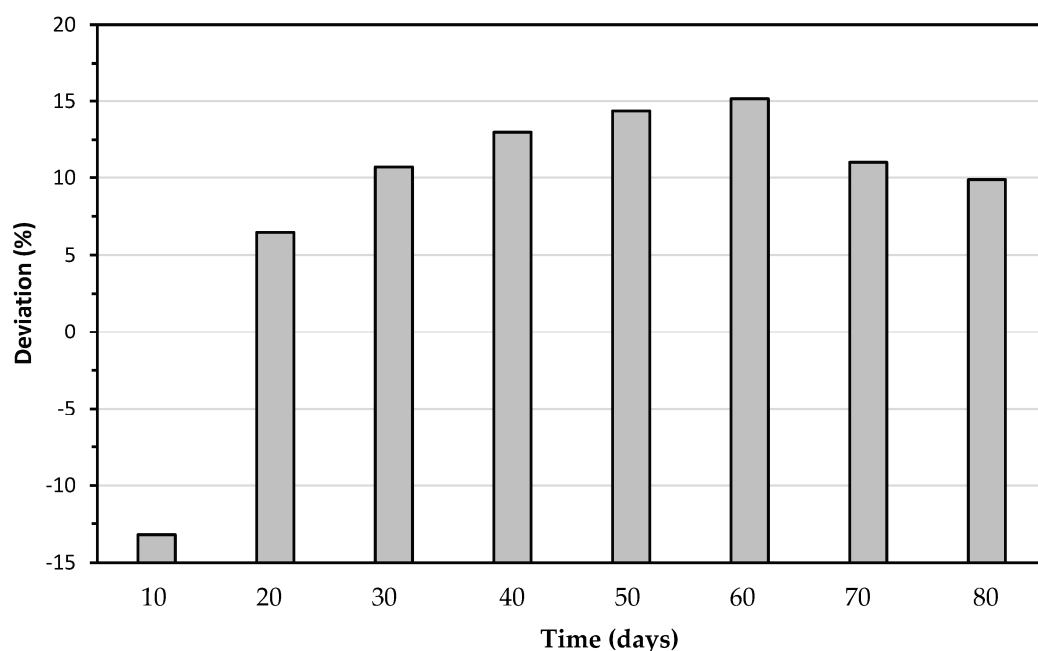


Figure 6. Comparison between FEM and field data.

The time-pattern of variation of the deviation between the numerical and field data is depicted from the bar chart in Figure 7. As observed, the deviation ranges between  $-13\%$  and  $15\%$ . The negative deviation, which occurs when the predicted value is less than the measured data, was observed in the initial construction phase of 0–15 days. Beyond this initial time, the deviation has been positive. The deviation was found to increase with increasing time, reaching its highest value at  $t = 60$  days.



**Figure 7.** Bar chart showing deviation between field data and FEM results at different time instances.

### 5.2. Discussion

The finite element predictions overestimate the field recorded settlements during the majority of the stages of construction. The reason may be attributed to the inability to correctly model the soil disturbances caused by the casting and installation of stone columns. Since stone columns are treated as embedded elements in soil prior to loading, the altered soil properties (in lieu of initial soil moduli and strength parameters) are not appropriately accounted for in analysis, as in case of field trials. Such deviation might occur due to a variety of issues, including (i) Smear effects due to the installation of stone columns are not considered. (ii) Interface between the stone columns and soil depends upon the method of installation and its shear properties can vary significantly.

As a result, the present study is unable to capture such interface zones despite accurately incorporating smear zone parameters.

### 5.3. Interpretations and Implications

The behavior of stone column reinforced soft clay deposit under embankment loading is a complex phenomenon with spatial and time dependency. Often, the theoretical results deviates to some extent with the field observation due to diversifying factors including stress concentration, clogging, lateral deformation, embankment arching, etc. [11].

The choice of stone column installation depends upon several factors discussed above. In the present scenario, the soft clay layer is extended to a relatively shallow depth; hence, the stone column embedded depth was decided as per the requirement of a fully penetrated granular reinforcement. The diameter was varied in a range of 0.8–1.2 m, while the spacing was kept at 2 m. The diameter and spacing were chosen based on construction convenience and area replacement ratio ( $A_r$ ). The values of  $A_r$  for different column diameters are presented in Table 3.

**Table 3.** Area replacement ratio.

Column Radii, $r_c$ (m)	Area Replacement Ratio, $A_r$ (%)
0.4	14.37
0.5	24.75
0.6	39.46

In the current field condition, the value of  $A_r$  is 14.37%, with a normalized column spacing of  $N = 2.82$  (where,  $N = r_e/r_c$ ). Therefore, the results obtained and the interpretations derived are contributory to these values. For more detailed investigations, more field studies with various values of column spacing and area replacement ratio should be conducted.

Furthermore, at the current site, the groundwater is situated in the vicinity of ground surface. Land subsistence is likely to occur under gradual groundwater depletion. Furthermore, land subsistence also takes place when rain water percolates down in the subsoil [50]. In the present situation, the field-based data were collected for the first 80 days from the commencement of construction. During this time, neither the groundwater table was depleted, nor did it rain heavily. Therefore, there was no land subsistence in the field. In addition, the magnitude of ground settlement under embankment loading is also influenced by drainage pattern in the field, plastic deformation of the columns, and effect of cyclic loading effects in case of transport infrastructure, etc. [14].

## 6. Summary and Conclusions

### 6.1. Summary

To investigate the load settlement characteristics of reinforced soft marine clay deposits, a group of stone column was installed at a site of Ballina, along the eastern coastal region of the state of New South Wales in Australia. The columns with varying diameter from 0.8 to 1.2 m were installed in square grid configuration. The areas surrounding the central columns were heavily instrumented and an earthen embankment of 15 m square at the base and 6 m at the top, with a height of 3 m, was constructed on the reinforced ground surface. The settlement pegs monitored the ground settlements at regular intervals. In order to carry out further study, a 2-dimensional plain strain finite element model was developed using the PLAXIS<sup>2D</sup> program.

### 6.2. Conclusions

The study revealed that the average ground settlement increased in a nonlinear manner as time passed. The average difference between measured and predicted average ground settlement was around 10%, while the latter values are being slightly higher. The deviation was found to be up to 15% maximum at a time interval of 60 days. The predicted ground settlements were lower than the measured values for the initial loading time of 0–15 days.

The observed model discrepancies could be explained by inability to account for installation effect and interface zones in the finite element analysis.

### 6.3. Significance and Novelty

Although remarkable past studies were conducted on stone column reinforced soft ground behavior including laboratory experimentations and theoretical analyses, appropriate field-based investigation is quite inadequate. The current study involves full-scale instrumented field trial in reinforced soft marine clay deposit. The load-settlement response of ground surface has been collected through field measurements. Subsequently, a robust finite element analysis has been carried out. The comparison of numerical results with the field measurements confirmed the validity of the proposed numerical model. Such a practical research is rarely available, which implies the novelty of the investigation.

### 6.4. Limitations and Recommendations

As discussed earlier, the observations and their interpretations are contributory to the specific values of normalized column spacing and area replacement ratio ( $N$  and  $A_r$ ) of 2.82 and 14.37%. Furthermore, the impervious bottom boundary condition because of the underlying stiff soil below the soft clay layer may not be valid in case the soft clay deposit overlies a sand bed.

For a generalized study and subsequent design recommendations, investigations with varying magnitudes of  $N$  and  $A_r$  and different bottom drainage conditions are desirable.

Moreover, a 3D finite element analysis capturing the appropriate field conditions would be more realistic.

Previously the authors analyzed the stress conditions induced in the column and the soil by explicit finite difference modeling and found both as time-dependent [12]. Currently, the authors are analyzing the stress and strain components in the soil-column system and their spatial and time pattern of variations through 3D finite element modeling. The computed results and the interpretations derived therefrom are expected to be published in the future.

**Author Contributions:** Conceptualization, S.B. and S.N.; methodology, S.B.; software, S.N.; validation, S.B. and S.N.; formal analysis, S.B. and S.N.; investigation, S.B. and S.N.; resources, S.B.; data curation, S.B. and S.N.; writing—original draft preparation, S.B.; writing—review and editing, S.N.; visualization, S.B.; supervision, S.B.; project administration, S.B. All authors have read and agreed to the published version of the manuscript.

**Funding:** The numerical research (FEM) received no external funding. However, the fieldworks and associated laboratory works were conducted with the financial and technical supports and assistances by University of Wollongong, National Soft Soil Testing Facility, Australia, the Australian Research Council, Coffey Geotechnics and Keller Ground Engineering.

**Institutional Review Board Statement:** Not applicable.

**Informed Consent Statement:** Not applicable.

**Data Availability Statement:** All data are available in the paper.

**Acknowledgments:** The authors thankfully acknowledge the financial and infrastructural supports received from the Australian Research Council, Coffey Geotechnics, Keller Ground Engineering, Soilwicks, Geomotions Australia, University of Wollongong and University of Technology Sydney to carry out the entire investigation. The support and advice received during the various stages of the research from Roger Lewis, Buddhima Indraratna, Cholachat Rujikiatkamjorn, Firman Siahaan, Cameron Neilson, Alan Grant, Richard Berndt and Bruce Perrin of University of Wollongong are also acknowledged.

**Conflicts of Interest:** The authors declare no conflict of interest.

## Notations

$A_r$ =	Area replacement ratio;
$c_{vr}$ =	Coefficient of radial consolidation;
$c_{vz}$ =	Coefficient of vertical consolidation;
$h_e$ =	Embankment height;
$K_0$ =	In-situ earth pressure coefficient;
$m_v$ =	Coefficient of volume compressibility of soil;
$n_s$ =	Stress concentration ratio;
$P_r$ =	Reduced parameters;
$P_u$ =	Undisturbed parameters;
$r_c$ =	Radius of stone columns;
$r_e$ =	Radius of influence;
$r, z, t$ =	Radial, depth and time coordinates;
$R_{int}$ =	Interface reduction coefficient;
$s$ =	Centre-to-centre spacing between stone columns;
$u$ =	Excess pore water pressure;
$\rho_a^t$ =	Average ground settlement;
$\sigma_c$ =	Vertical stress on column;
$\sigma_s$ =	Vertical stress on soil;

## References

1. Wang, G. Consolidation of Soft soil foundations reinforced by stone columns under time dependent loading. *J. Geotech. Geoenviron. Eng.* **2009**, *135*, 1922–1931. [[CrossRef](#)]
2. Fatahi, B.; Basack, S.; Premananda, S.; Khabbaz, H. Settlement prediction and back analysis of Young's modulus and dilation angle of stone columns. *Aust. J. Civ. Eng.* **2012**, *10*, 67–80. [[CrossRef](#)]
3. Almeida, M.S.; Hosseinpour, I.; Riccio, M.; Alexiew, D. Behaviour of geotextile-encased granular columns supporting test embankments on soft deposits. *J. Geotech. Geoenviron. Eng.* **2015**, *141*, 04014116. [[CrossRef](#)]
4. Fahmi, S.K.; Kolosov, E.S.; Fattah, M.Y. Behavior of different materials for stone column construction. *J. Eng. Appl. Sci.* **2019**, *14*, 1162–1168.
5. Han, J.; Ye, S.L. Simplified method for consolidation rate of stone column reinforced foundations. *J. Geotech. Geoenviron. Eng.* **2001**, *127*, 597–603. [[CrossRef](#)]
6. Fattah, M.Y.; Shlash, K.T.; Al-Waily, M.J. Experimental evaluation of stress concentration ratio of model stone columns strengthened by additives. *Int. J. Phys. Model. Geotech.* **2013**, *13*, 79–98. [[CrossRef](#)]
7. Fattah, M.Y.; Zabar, B.S.; Hassan, H.A. Soil arching analysis in embankments on soft clays reinforced by stone columns. *Struct. Eng. Mech.* **2015**, *56*, 507–534. [[CrossRef](#)]
8. Han, J.; Ye, S.L. A theoretical solution for consolidation rates for stone column reinforced foundations accounting for smear and well resistance effects. *Int. J. Geomech.* **2002**, *2*, 135–151. [[CrossRef](#)]
9. Sondermann, W. Ground improvement as alternative to piling—effective design solutions for heavily loaded structures. In Proceedings of the 2nd GeoMEast International Congress and Exhibition on Sustainable Civil Infrastructures, Cairo, Egypt, 24–28 November 2018.
10. Weber, T.M.; Plotze, M.; Laue, J.; Peschke, G.; Springman, S.M. Smear zone identification and soil properties around stone columns constructed in-flight in centrifuge model tests. *Géotechnique* **2010**, *60*, 197–206. [[CrossRef](#)]
11. Indraratna, B.; Basack, S.; Rujikiatkamjorn, C. Numerical solution to stone column reinforced soft ground considering arching, clogging and smear effects. *J. Geotech. Geoenviron. Eng.* **2013**, *139*, 377–394. [[CrossRef](#)]
12. Basack, S.; Indraratna, B.; Rujikiatkamjorn, C.; Siahaan, F. Modeling the stone column behavior in soft ground with special emphasis on lateral deformation. *J. Geotech. Geoenviron. Eng.* **2017**, *143*, 04017016. [[CrossRef](#)]
13. Basack, S.; Indraratna, B.; Rujikiatkamjorn, C.; Siahaan, F. Stone column–stabilized soft-soil performance influenced by clogging and lateral deformation: Laboratory and numerical evaluation. *Int. J. Geomech.* **2018**, *18*, 04018058. [[CrossRef](#)]
14. Basack, S.; Indraratna, B.; Rujikiatkamjorn, C. Modeling the performance of stone column reinforced soft ground under static and cyclic loads. *J. Geotech. Geoenviron. Eng.* **2016**, *142*, 04015067. [[CrossRef](#)]
15. Basack, S.; Indraratna, B.; Rujikiatkamjorn, C. Analysis of the behaviour of stone column stabilized soft ground supporting transport infrastructure. *Procedia Eng.* **2016**, *143*, 347–354. [[CrossRef](#)]
16. Basack, S.; Nimbalkar, S. Numerical solution of single pile subjected to torsional cyclic load. *Int. J. Geomech.* **2017**, *17*, 04017016. [[CrossRef](#)]
17. Fattah, M.Y.; Majeed, Q.G. A Study on the behaviour of geogrid encased capped stone columns by the finite element method. *Int. J. Geomate* **2012**, *3*, 343–350. [[CrossRef](#)]
18. Fattah, M.Y.; Zabar, B.S.; Hassan, H.A. An experimental analysis of embankment on stone columns. *J. Eng.* **2014**, *20*, 62–84.
19. Remadna, A.; Benmebarek, S.; Benmebarek, N. Numerical analyses of the optimum length for stone column reinforced foundation. *Int. J. Geosynth. Ground Eng.* **2020**, *6*, 1–12. [[CrossRef](#)]
20. Ng, K.S. Numerical study on bearing capacity of single stone column. *Int. J. Geo-Eng.* **2018**, *9*, 1–10. [[CrossRef](#)]
21. Thakur, A.; Rawat, S.; Gupta, A.K. Experimental study of ground improvement by using encased stone columns. *Innov. Infrastruct. Solut.* **2020**, *6*, 1–13. [[CrossRef](#)]
22. Christoulas, S.; Bouckovalas, G.; Giannaros, C. An experimental study on model stone columns. *Soils Found.* **2000**, *40*, 11–22. [[CrossRef](#)] [[PubMed](#)]
23. Bruno, T.L.; Marcio, S.S.A.; Iman, H. Field measured and simulated performance of a stone columns-strengthened soft clay deposit. *Int. J. Geotech. Eng.* **2022**, *16*, 776–785.
24. Pandey, B.K.; Rajesh, S.; Chandra, S. Time-dependent behavior of embankment resting on soft clay reinforced with encased stone columns. *Transp. Geotech.* **2022**, *36*, 100809. [[CrossRef](#)]
25. Ashour, S.; Ghataora, G.; Jefferson, I. Behaviour of model stone column subjected to cyclic loading. *Transp. Geotech.* **2022**, *35*, 100777. [[CrossRef](#)]
26. Hamzh, A.; Mohamad, H.; Yusof, M.H.B. The effect of stone column geometry on soft soil bearing capacity. *Int. J. Geotech. Eng.* **2019**, *16*, 200–210. [[CrossRef](#)]
27. Basack, S.; Goswami, G.; Khabbaz, H.; Karakouzian, M.; Baruah, P.; Kalita, N. A Comparative study on soil stabilization relevant to transport infrastructure using bagasse ash and stone dust and cost effectiveness. *Civ. Eng. J.* **2021**, *7*, 1947–1963. [[CrossRef](#)]
28. Saxena, S.; Roy, L.B. The effect of geometric parameters on the strength of stone columns. *Eng. Technol. Appl. Sci. Res.* **2022**, *12*, 9028–9033. [[CrossRef](#)]
29. Riccio, F.M.V.; Almeida, M.S.S.; Vasconcelos, S.M.; Pires, L.G.S.; Nicodemos, R.L.F. Embankment supported by low area replacement ratio stone columns, monitoring and numerical studies. *KSCE J. Civ. Eng.* **2022**, *26*, 619–629. [[CrossRef](#)]

30. Doherty, J.P.; Gourvenec, S.; Gaone, F.M.; Pineda, J.A.; Kelly, R.B.; O'Loughlin, C.D.; Cassidy, M.J.; Sloan, S.W. A novel web based application for storing, managing and sharing geotechnical data, illustrated using the national soft soil field testing facility in Ballina, Australia. *Comput. Geotech.* **2017**, *93*, 3–8. [[CrossRef](#)]
31. Wollongbar Planning and Environmental Study. Technical Report, NSW Spatial Services. 2017. Available online: <https://ballina.nsw.gov.au/files/Wollongbar-Planning-and-Environmental-Study.pdf> (accessed on 1 February 2022).
32. Pineda, J.A.; Suwal, L.P.; Kelly, R.B.; Bates, L.; Sloan, S.W. Characterisation of Ballina clay. *Géotechnique* **2016**, *66*, 556–577. [[CrossRef](#)]
33. Pineda, J.A.; Kelly, R.B.; Suwal, L.P.; Bates, L.; Sloan, S.W. The Ballina soft soil field testing facility. *AIMS Geosci.* **2019**, *5*, 509–534. [[CrossRef](#)]
34. Xie, Z. Influence of Stone Column Installation on Consolidation Characteristics of Soft Clay. Bachelor's Thesis, School of Civil, Mining and Environmental Engineering, University of Wollongong, Wollongong, Australia, 12 June 2016.
35. Bharadwaj, S. Smear Zone Characterisation of Stone Column Reinforced Soft Ground. Master's Thesis, School of Civil, Mining and Environmental Engineering, University of Wollongong, Wollongong, Australia, 21 December 2016.
36. Basack, S.; Indraratna, B.; Rujikiatkamjorn, C. Effectiveness of stone column reinforcement for stabilizing soft ground with reference to transport infrastructure. *Geotech. Eng. J.* **2018**, *49*, 8–14.
37. Basack, S.; Nimbalkar, S.; Karakouzian, M.; Bharadwaj, S.; Xie, Z.; Krause, N. Field installation effects of stone columns on load settlement characteristics of reinforced soft ground. *Int. J. Geomech.* **2022**, *22*, 04022004. [[CrossRef](#)]
38. Brinkgreve, R.B.J.; Kumarswamy, S.; Swolfs, W.M. *PLAXIS 2D (Version 2017) Reference Manual*; Delft University of Technology and PLAXIS B.V.: Delft, The Netherlands, 2017.
39. Basack, S.; Nimbalkar, S. Measured and predicted response of pile groups in soft clay subjected to cyclic lateral loading. *Int. J. Geomech.* **2018**, *18*, 04018073. [[CrossRef](#)]
40. Chen, Q.; Li, Y.; Hu, Z.; Xu, C.; Basack, S.; Ke, W. Utilization of horizontally buried hollow pipes for ground vibration mitigation in public transport infrastructure: An innovative technique. *Int. J. Geomech.* **2022**, *22*, 04022215. [[CrossRef](#)]
41. Weber, T.M. Centrifuge modeling of ground improvement under embankments. *Pollack Periodica* **2006**, *1*, 3–15. [[CrossRef](#)]
42. Marto, A.; Moradi, R.; Helmi, F.; Latifi, N. Performance analysis of reinforced stone columns using finite element method. *Electron. J. Geotech. Eng.* **2013**, *18*, 315–323.
43. Castro, J. Modeling stone columns. *Materials* **2017**, *10*, 782. [[CrossRef](#)] [[PubMed](#)]
44. Li, H. Equivalent plane strain model of stone column reinforced foundation. *IOP Conf. Ser. Earth Environ. Sci.* **2021**, *634*, 012153. [[CrossRef](#)]
45. Nimbalkar, S.; Basack, S. Pile group in clay under cyclic lateral loading with emphasis on bending moment: Numerical modelling. *Mar. Georesources Geotechnol.* **2022**, *41*, 269–284. [[CrossRef](#)]
46. Keller. *Vibro Ground Improvement*; Keller Ground Engineering: Mumbai, India, 2022.
47. Shehata, H.F.; Sorour, T.M.; Fayed, A.L. Effect of stone column installation on soft clay behaviour. *Int. J. Geotech. Eng.* **2021**, *15*, 530–542. [[CrossRef](#)]
48. Barron, B.A. Consolidation of fine grained soil by drain wells. *Trans. ASCE* **1948**, *113*, 712–748.
49. Basack, S.; Karami, M. and Karakouzian, M. Pile-soil interaction under cyclic lateral load in loose sand: Experimental and numerical evaluations. *Soil Dyn. Earthq. Eng.* **2022**, *162*, 107439. [[CrossRef](#)]
50. Jiang, H.; Zhang, J.; Liu, Y.; Li, J.; Fang, Z.N. Does flooding get worse with subsiding land? Investigating the impacts of land subsidence on flood inundation from Hurricane Harvey. *Sci. Total Environ.* **2023**, *865*, 161072. [[CrossRef](#)]

**Disclaimer/Publisher's Note:** The statements, opinions and data contained in all publications are solely those of the individual author(s) and contributor(s) and not of MDPI and/or the editor(s). MDPI and/or the editor(s) disclaim responsibility for any injury to people or property resulting from any ideas, methods, instructions or products referred to in the content.